Kinetics of growing and coalescing droplets

1992 J. Phys. A: Math. Gen. 25 705

(http://iopscience.iop.org/0305-4470/25/4/011)

J. Phys. A: Math. Gen. **25** (1992) 705–713. Printed in the UK

Kinetics of growing and coalescing droplets

K Pesz† and G J Rodgers

Department of Physics, Brunel University, Uxbridge, Middlesex UB8 3PH, UK

Received 1 August 1991, in final form 24 October 1991

Abstract. A class of mean field models for the patterns formed by growing and coalescing droplets on a line is introduced and solved. All the models are found to have a scale-invariant regime where the patterns are self-similar in time.

1. Introduction

The phenomenon of the growth and coalescence of fluid on a surface, such as the condensation of vapour on a cold surface, is one of the most commonly observed in nature. The patterns formed by the droplets on the surface, referred to as breath figures, have been the subject of a number of experimental [1, 2] and theoretical [3–6] studies.

As a result of this work, a number of different time regimes have been identified for this process [1].

In the first regime the droplets nucleate and grow. The distance between the droplets is very much larger than their size and no coalescence takes place.

In the second regime the droplets start to coalesce and new droplets are formed. If the droplets are assumed to be hyperspherical, the radius of the new droplet, R, is given by

$$R = (R_1^D + R_2^D)^{1/D}$$

where D is the dimension of the droplets and R_1 and R_2 are the radii of the original droplets. This relation ensures that mass is conserved. In this regime the distances between the droplets and their radii are the same order of magnitude, the patterns are self-similar in time and the area of the surface covered by the droplets approaches a constant value.

In the third regime, droplets nucleate in the spaces left by the coalescing droplets and, depending on the wetting properties of the surface, the droplets may form a uniform fluid.

A simplified one-dimensional model has recently been introduced [3] to model the kinetics of breath figures in the first and second time regimes described above. This model comprises a number of equally sized spherical droplets on a line. The droplets are growing in time, but at the same rate, so that they all have the same radius. When two neighbouring droplets touch, a new droplet of the same radius is formed, centred

† On leave from the Technical University of Wrocław, Institute of Organic and Physical Chemistry, Wyspianskiego 27, 51-370 Wrocław, Poland.

0305-4470/92/040705+09$04.50

on the point where the two original droplets touched. The model can be regarded as D-dimensional droplets on a $1-d$ surface in the $D\to\infty$ limit.

As all the droplets have the same size in this model, the rate of growth of the droplets is unimportant and the distribution of distances between the droplets is the only relevant quantity. Hence, this model may be visualized as a number of points on a line, the distance between neighbouring points corresponding to the distance between neighbouring droplets. The dynamics are modelled by finding the two points which are closest together and replacing them by a single point midway between them. Consequently, this model may be simulated by generating a sequence of random bonds, finding the shortest one, removing it and adding half its length to the two bonds either side. The next smallest bond is found and the procedure is repeated.

In the mean field version of this model, introduced by Derrida *et al* [3], the correlation between bonds is neglected and the two halves of the shortest bond are added to two bonds chosen at random. This model can be solved analytically.

In this paper we introduce a generalized version of this mean field model. A natural extension of their procedure arises because there is no reason why every bond removed has to be divided into two parts of the same length. Therefore, we have examined the extent to which the stationary solutions are changed by a more general 'cut in n and paste'. Derrida *et al* considered the case $n=1$ in [4], where the $n=1$ model was found to be exactly the same as its $1-d$ counterpart. The mean field models (with $n>2$) which we consider here do not have finite-dimensional counterparts.

Neither does the growth have to be symmetric. We have looked at how the stationary, self-similar pattern at long times survives when a given bond is split into n parts and the growth proceeds by addition of $m_1, m_2, m_3, \ldots, m_k$ parts to k other bonds where

$$\sum_{i=1}^{k} m_i = n. \tag{1}$$

The result of these studies show that these modifications, apart from giving rise to minor qualitative changes to the stable distribution function, cannot destroy the stability of the stationary patterns of bonds.

2. The models

Firstly, we will examine the model in which the shortest bond is cut into n pieces and these are added individually to n bonds selected at random. This corresponds to $m_i=1$ and $k=n$ in equation (1).

If $Ng_t(h)$ is the number of bonds of length between h and $h+\delta h$ at time t and in the time interval $(t, t+\delta t)$ all the bonds of length between h_0 and $h_0+\delta h$ are removed, then $g_t(h)$ obeys the kinetic equation

$$g_{t+\delta t}(h) = g_t(h) + n\delta h g_t(h_0)\left[g_t\left(h-\frac{1}{n}h_0\right)\theta\left(h-\frac{n+1}{n}h_0\right) - g_t(h)\right]\left(\int_{h_0}^{\infty} g_t(\tilde{h})\,\mathrm{d}\tilde{h}\right)^{-1}. \tag{2}$$

The first term inside the brackets corresponds to the bonds added to at time t and the second term corresponds to the bonds removed. The normalization must be included because, although the total length of the bonds is a conserved quantity, the number of bonds is reduced at each time step. The θ-function is a consequence of there being no bond shorter than h_0 at any instant of time, t.

The fraction of lengths between h and $h+\delta h$ at time t is given by

$$f_t(h)=\frac{g_t(h)}{\int_{h_0}^{\infty} g_t(\tilde{h})\,\mathrm{d}\tilde{h}} \tag{3}$$

and substituting $f_t(h)$ into (2) and using

$$\int_{h_0+\delta h}^{\infty} g_{t+\delta t}(\tilde{h})\,\mathrm{d}\tilde{h}=\int_{h_0}^{\infty} g_t(\tilde{h})\,\mathrm{d}\tilde{h}-\delta h g_t(h_0) \tag{4}$$

gives

$$f_{t+\delta t}(h)=f_t(h)+\delta h f_t(h_0)\left[nf_t\left(h-\frac{1}{n}h_0\right)\theta\left(h-\frac{n+1}{n}h_0\right)-(n-1)f_t(h)\right]. \tag{5}$$

The shortest bond h_0 is a natural length scale in this problem so it is convenient to introduce a function $F(x, t)$ defined for $x>1$ by

$$F(x, t)=h_0 f_t(xh_0). \tag{6}$$

$F(x, t)$ obeys the differential equation

$$\frac{\partial F(x, t)}{\partial t}=F(x, t)+x\frac{\partial F(x, t)}{\partial x}+F(1, t)\left[nF\left(x-\frac{1}{n}, t\right)\theta\left(x-\frac{n+1}{n}\right)-(n-1)F(x, t)\right]. \tag{7}$$

Here we have assumed that $h_0\delta t/\delta h=1$. This represents the relationship between the minimum length and real time, which is irrelevant for this model.

The mean coverage of the line at time t is given by

$$C(t)=\frac{h_0}{\int_{h_0}^{\infty}\tilde{h}f_t(\tilde{h})\,\mathrm{d}\tilde{h}}=\frac{1}{\int_1^{\infty}xF(x, t)\,\mathrm{d}x}. \tag{8}$$

By introducing the Laplace transform

$$\phi(p, t)=\int_1^{\infty}F(x, t)\,\mathrm{e}^{-px}\,\mathrm{d}x \tag{9}$$

the whole problem is reduced to solving the differential equation

$$\frac{\partial\phi(p, t)}{\partial t}=F(1, t)\left[n\exp\left(-\frac{p}{n}\right)-(n-1)\right]\phi(p, t)-F(1, t)\,\mathrm{e}^{-p}-p\frac{\partial\phi(p, t)}{\partial p} \tag{10}$$

with some given initial condition, $F(x, 0)$ or $\phi(p, 0)$. We were unable to solve this equation in general; however, the stationary solutions, controlled by the parameter $F(1)$, are given by

$$\phi(p)=F(1)\int_p^{\infty}\frac{\mathrm{d}t}{t}\exp\left(-t+F(1)\int_p^{t}\frac{(n-1)-n\exp(-u/n)}{u}\,\mathrm{d}u\right). \tag{11}$$

This result is the same as that obtained in [3] for the $n=2$ model and in [4] for $n=1$. For the long times the coverage of the line by the droplets is given by

$$C(\infty)=\frac{1}{\bar{x}}=\frac{-1}{\phi'(0)}. \tag{12}$$

Expanding $\phi(p)$ for small p gives $\phi(p)\approx 1-p^{F(1)}$ and hence the only value of $F(1)$ that gives a finite coverage is $F(1)=1$. $F(1)>1$ gives $x=0$ and can be ruled out

completely as x is always positive. $F(1)<1$ gives $x=\infty$ and implies that $F(x)$ decays more slowly than $1/x^2$. This situation may occur if the initial distribution of bonds decays sufficiently slowly. We attempted to observe this effect numerically by selecting bonds from various appropriate distributions and performing the dynamics. As might be expected, with the size of system available to us it was difficult to discern when the system had converged to a stable time-independent distribution.

Consequently, all simulations of the models or all iterations of equation (5) were with initial distributions which decayed quickly for large x and produced a stable distribution with $F(1)=1$. In addition, iterations of equation (7), which assumed $F(1)=1$, produced stable distributions which coincided with the results of simulations.

Under the assumption that $F(1)=1$ the mean value of x is given by

$$\bar{x}=\int_0^\infty \frac{dt}{t^2}\left[1-\exp\left(-t+n\int_0^t \frac{1-\exp(-u/n)}{u}\,du\right)\right]. \tag{13}$$

The coverage and mean values of x are given for various values of n in table 1.

Notice that $\phi(p)\to\exp(-p)$, $F(x)\to\delta(x-1)$ and $x=1$ as $n\to\infty$ in equation (11) so that the stationary solution which the system arrives at is one in which every bond is of the same length. As $n\to 0$, $F(x)\to 1/x^2$ which gives an infinite mean bond length.

Table 1. The coverage and mean values of x for various values of n.

n	$\bar{x}$	$C(\infty)$
1	1.78	0.56
2	1.57	0.64
3	1.47	0.68
4	1.42	0.70
5	1.37	0.73
10	1.23	0.81

At this point it is useful to note how these equations are changed by considering the more general addition rule described in the introduction. Here the rule is that the shortest bond is divided into n parts and $m_1, m_2, m_3, \ldots, m_k$ of these parts are added to k other bonds. Under these conditions equation (7) is changed to

$$\frac{\partial F(x,t)}{\partial t}=F(x,t)+x\frac{\partial F(x,t)}{\partial x}+F(1,t)$$
$$\times\left[\sum_{i=1}^{k} F\left(x-\frac{m_i}{n},t\right)\theta\left(x-\frac{n+m_i}{n}\right)-(k-1)F(x,t)\right] \tag{14}$$

and the Laplace transform of the stationary solution becomes

$$\phi(p)=F(1)\int_p^\infty \frac{dt}{t}\exp\left(-t+F(1)\int_p^t \frac{(k-1)-\Sigma_{i=1}^{k}\exp(-m_iu/n)}{u}\,du\right). \tag{15}$$

3. Simulations and numerical solutions

Figures 1 and 2 show $F(x,t)$ obtained by the simulation of models $n=3$ and $n=4$. These were performed by generating 300 000 random numbers between 0 and 1 and

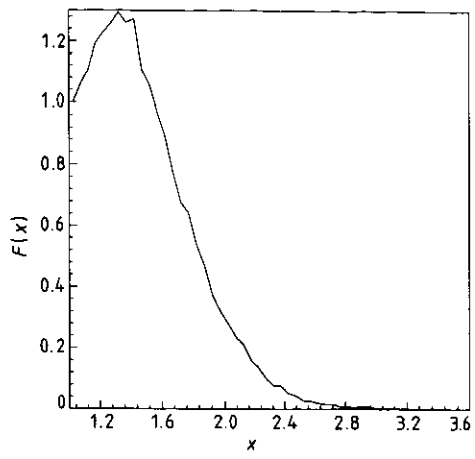

Figure 1. $F(x, t)$ for the $n = 3$ model obtained by taking 300 000 random numbers between 0 and 1 and running the simulation of the model until only 40 000 bonds remained.

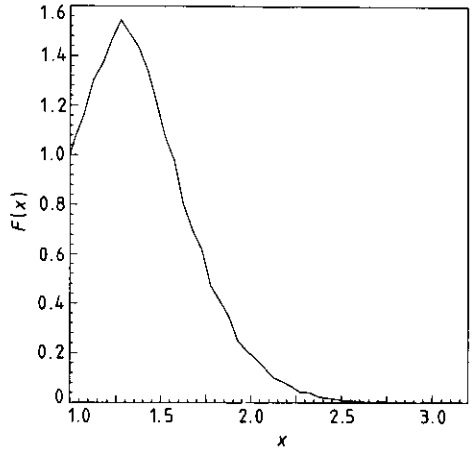

Figure 2. Same as figure 1 for the $n = 4$ model.

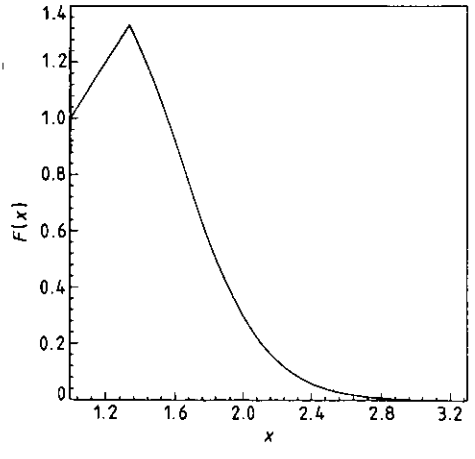

Figure 3. The stationary solution $F(x)$ of the $n = 3$ model obtained by iterating equation (7) with $F(1) = 1$.

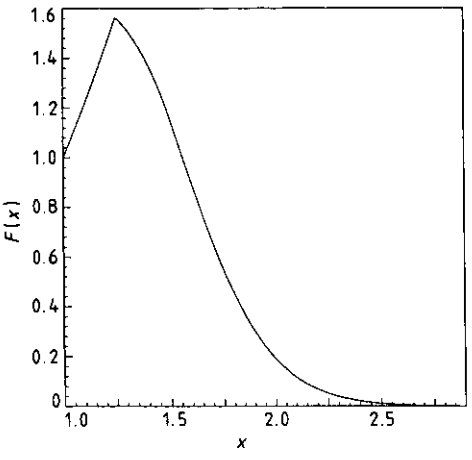

Figure 4. Same as figure 3 for the $n = 4$ model.

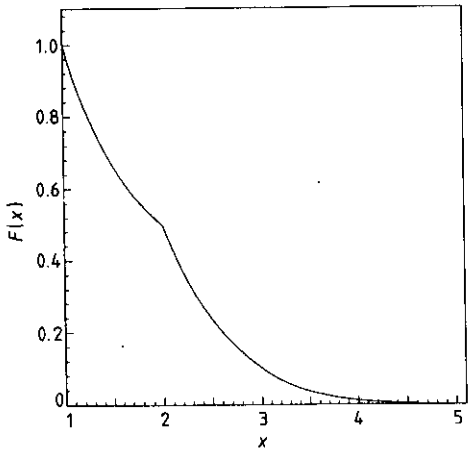

Figure 5. Same as figure 3 for the $n = 1$ model.

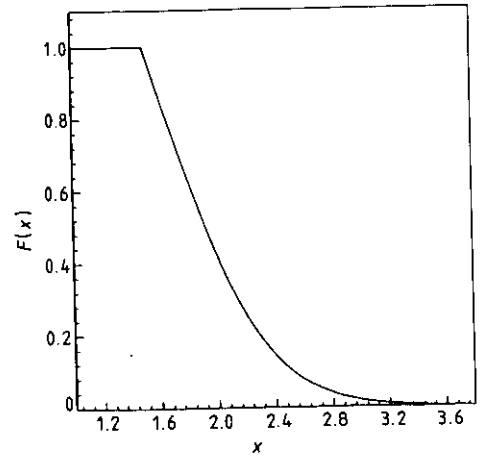

Figure 6. Same as figure 3 for the $n = 2$ model.

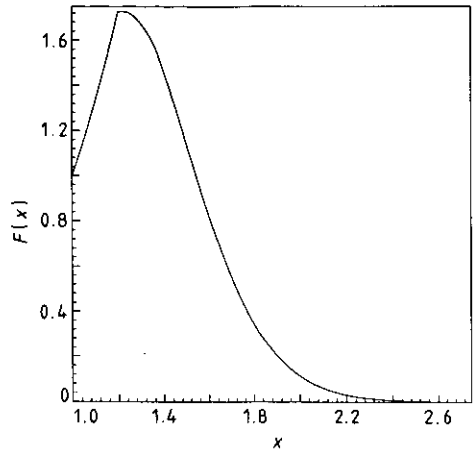

Figure 7. Same as figure 3 for the $n = 5$ model.

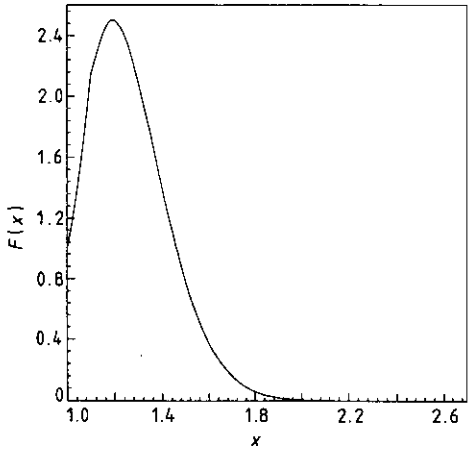

Figure 8. Same as figure 3 for the $n = 10$ model.

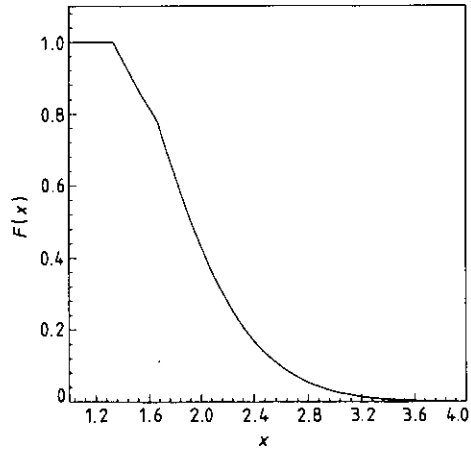

Figure 9. The stationary solution $F(x)$ obtained by iterating equation (14) with $m_1 = 2$, $m_2 = 1$, $n = 3$ and $k = 2$.

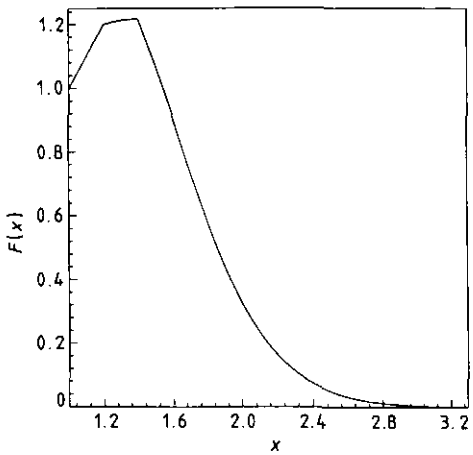

Figure 10. Same as figure 9 with $m_1 = m_2 = 2$, $m_3 = 1$, $n = 5$ and $k = 3$.

removing the shortest bonds under the rules described above until only 40 000 bonds remained. Simulations performed for slightly larger systems over longer times produced identical results, indicating that the distribution of droplets is self-similar for large times. In figures 3 and 4 the results of iterating equation (7) are shown for $n = 3$ and $n = 4$. The graphs are entirely consistent with figures 1 and 2. The results of iterations of equation (7) for $n = 1$, 2, 5 and 10 are shown for the comparison in figures 5–8. In all these graphs there is a discontinuity at $x = (n+1)/n$ caused by the θ step function in equation (7). As n increases the discontinuity becomes less pronounced.

Simulations were also performed of the generalized model for various values of n and m_i, $i = 1, k$. These always produced stable self-similar solutions. In figure 9, the result of the iteration of equation (14) with $m_1 = 2$, $m_2 = 1$, $k = 2$ and $n = 3$ is shown. These values of the parameters correspond to the process of dividing the shortest bond into three and adding two parts to one bond chosen at random and one part to another. In figure 10 the result of the iteration with $m_1 = m_2 = 2$, $m_3 = 1$, $k = 3$ and $n = 5$ is shown. This is the process of dividing the shortest bond into five and adding two parts to two different bonds and the remaining part to a third. Notice that in these last two figures there are now two discontinuities arising from the two step functions in equation (14).

4. Conclusions

We have introduced and solved a set of mean field models which reproduce qualitatively the behaviour of experimental and numerical results from more complicated systems. The shapes of the stable distributions obtained in the scale-invariant regime are crucially dependent on the way in which the distributions decay at infinity. Changes in the dynamic rule have little effect on this behaviour.

Another feature of the stable distributions is that although the tail of long bonds appears for every n, the density of bonds near $(1+1/n)h_0$ increases with n and the tail becomes steeper. Thus, although the overall picture of self-similar distributions remains, the system of bonds tends to be more homogeneous for large n. This agrees well with an observation of van Dongen and Ernst [7] that, for singular kernels of coagulation frequencies, the size spectrum peaks around the mean length. This property cannot be destroyed by an asymmetric growth within the mean field model.

Acknowledgment

One of us (KP) would like to thank the Science and Engineering Research Council for financial support.

References

[1] Beysens D and Knobler C M 1986 *Phys. Rev. Lett.* **57** 1433
[2] Wright H, Muralidhar R, Tobin T and Ramkrishna D 1990 *J. Stat. Phys.* **61** 843
[3] Derrida B, Godreche C and Yekutieli I 1990 *Europhys. Lett.* **12** 385
[4] Derrida B, Godreche C and Yekutieli I 1991 *Phys. Rev.* A **44** 6241
[5] Meakin P and Family F 1989 *J. Phys. A: Math. Gen.* **22** L225
[6] Baram A and Kutasov D 1989 *J. Phys. A: Math. Gen.* **22** L251
[7] van Dongen P G J and Ernst M H 1988 *J. Stat. Phys.* **50** 295